11th International Conference on Fracture Mechanics of Concrete and Concrete Structures
FraMCoS-11
J. M. Chandra Kishen, A. Ramaswamy, S. Ray and R. Vidyasagar (Eds.)
https://doi.org/10.21012/FC11.092377

MACRO- AND MESOSTRUCTURAL PARAMETERS FOR ESTIMATING FATIGUE LIFE IN HIGH-PERFORMANCE FIBER-REINFORCED CONCRETE IN BENDING

ÁLVARO MENA-ALONSO[1], GREGOR GEBUHR[2], MIGUEL A. VICENTE[1], STEFFEN ANDERS[2], JESÚS MÍNGUEZ[1] AND DORYS C. GONZÁLEZ[1]

[1] Department of Civil Engineering, University of Burgos (UBU)
C. Villadiego s/n, 09001 Burgos, Spain
e-mail: eps@ubu.es, www.ubu.es

[2] Institute for Structural Engineering, University of Wuppertal (BUW)
Pauluskirchstr. 11, 42285 Wuppertal, Germany
e-mail: ikiboffice@uni-wuppertal.de, www.uni-wuppertal.de

Key words: flexural fatigue, fiber-reinforced concrete, cyclic creep curve, microCT.

Abstract: Fatigue in concrete is characterized by a great variability of results in terms of fatigue life. Therefore, it is necessary to look for parameters to explain this dispersion. In this work, two types of parameters are proposed to estimate the flexural fatigue life in steel fiber-reinforced concrete. On the one hand, macroscopic damage indicators based on cyclic creep curves. On the other hand, parameters related to the arrangement of the fibers inside the matrix. The results show that the former predict more accurately the dispersion of N. However, the latter have the advantage that they are determined without the need to inflict prior damage to concrete.

1 INTRODUCTION

One of the main issues when studying fatigue in concrete is the wide dispersion of results in terms of number of cycles to failure. In experimental campaigns it is common that the fatigue life in series of identical specimens subjected to the same stress levels can vary by two or more orders of magnitude.

The practical consequence of this fact is that structural codes are very conservative, imposing wide safety margins in fatigue design. Nowadays, this is beginning to be a cause for concern, since, with the improvement of concrete, structures are becoming increasingly slender and therefore more susceptible to cyclic loads produced by wind, traffic, etc. A clear example is concrete wind turbine towers, whose design is conditioned by wind fatigue.

In order to try to explain the dispersion of fatigue life, macrostructural parameters can be used. Cyclic creep curves represent the strain at the maximum stress level S_{max} vs. the number of cycles (Figure 1). These curves have a characteristic S-shape, being divided into 3 stages. Stage (II) is the most extensive and governs the evolution of fatigue damage. It is characterized by an approximately constant increase in strain with the number of cycles. Sparks & Menzies [1] showed that there is a very good correlation between the logarithms of N and the slope of stage (II), called secondary strain rate ($d\varepsilon/dn$). It is found that, the higher $d\varepsilon/dn$, the lower N. Therefore, this macroscopic damage parameter is able to explain why the fatigue life is different in apparently identical specimens.

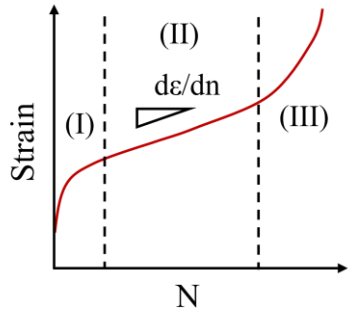

Figure 1: Cyclic creep curve in compressive fatigue.

Numerous works have verified this relationship, demonstrating that it is a property of the material, and therefore independent of the test parameters [2,3].

In the particular case of flexural fatigue, some authors point out that this relationship is also fulfilled, so that there is a certain correlation between the secondary crack opening rate (dCMOD/dn) and fatigue life [4,5]. However, publications on this subject are scarce, so it is interesting to study cyclic creep curves in flexural fatigue in greater depth.

Alternatively, it is likely that the scatter of fatigue life in equal specimens is due to the fact that the specimens are not actually identical. Because of the heterogeneous nature of concrete, small variations in its mesostructure may result in a different macroscopic response. In steel fiber-reinforced concrete (SFRC) subjected to flexural fatigue, fibers largely dominate the fracture behavior. Consequently, it is of great interest to analyze the main parameters characterizing the fiber arrangement (orientation, position, etc.), assessing their impact on fatigue response.

In this sense, many investigations study the influence of fiber position and orientation on the static response of concrete, such as compressive or flexural strength [6–8]. However, in fatigue the works are scarcer [6–10].

One of the most common techniques to explore the concrete mesostructure is micro-computed tomography (microCT). This technique is based on the different X-ray absorption of the matter depending on its density. There are a good number of publications that apply microCT for the analysis of the distribution of fibers within the concrete matrix [8–11]. In addition, in recent years this technology is being used for the study of concrete porosity.

The aim of this work is to study the dispersion of fatigue life in SFRC subjected to flexural fatigue. Specifically, three series of specimens with different fiber contents have been tested. Several parameters that can explain the variability of the results have been analyzed. On the one hand, macroscopic damage parameters based on cyclic creep curves. On the other hand, parameters related to fiber arrangement, obtained from microCT scans.

The paper is structured as follows. Section 2 describes the experimental program; Section 3 presents the results and discussion; and finally, Section 4 contains the conclusions.

2 EXPERIMENTAL PROGRAM

2.1 Materials and specimens

This research has dealt with SFRC with three different fiber contents: 0.3% (low), 0.6% (medium) and 1% (high). The lowest corresponds to the minimum amount recommended by the manufacturer.

The concrete produced has high strength and is self-compacting. The three mixes were designed so that the only difference between them was the fiber content.

Table 1 contains the dosages of the three series. Portland cement CEM I 52.2 R was used. The aggregates were silica sand 0/4 and silica gravel 4/10, as well as limestone filler. The additives included were superplasticizer MasterEase 5025 and nanosilica MasterRoc MS 685 (BASF, Ludwigshafen am Rhein, Germany). Finally, Dramix RC-80/30-CP steel fibers (Bekaert, Zwevegem, Belgium) were added. They are 30 mm long hooked-end fibers with an aspect ratio of 78.9.

Table 1: Concrete mixtures (in kg/m^3).

Component	A1	A2	A3
Cement	400		
Coarse aggregate	538		
Fine aggregate	847		
Filler	449		
Water	160		
Superplasticizer	16		
Nanosilica	20		
Steel fibers	23.6	47.1	78.5

A total of 16 prismatic specimens with dimensions of 75x75x300 mm per series were cast. A 12.5 mm notch was made in the central section of all of them. These specimens are homothetic to those indicated in the standard flexural strength test (EN 14651:2007), and have the advantage that their size is small enough to be scanned by microCT. In addition, 8 cylindrical specimens of 150x300 mm were manufactured in each series to perform concrete characterization tests.

All specimens were kept in a curing chamber at 20°C and 95% humidity for one year. Thus, it can be assumed that the variation in concrete strength is residual and therefore has no impact on the fatigue results.

2.2 Concrete characterization

Concrete characterization tests were carried out in both fresh and hardened states.

In fresh state, it was verified that all the series meet the condition of self-compactness, since the diameter of the extended concrete (d_f) in the slump flow test (EN 12350-8:2019) ranges between 770 mm (series A1) and 650 mm (series A3).

On the other hand, just before the fatigue tests, compressive strength (EN 12390-3:2019) and modulus of elasticity (EN 12390-13:2013) tests were performed. The average compressive strength in all series is 106.7 ± 2.2 MPa. The overall mean modulus of elasticity is 45.4 ± 0.9 GPa. It is observed that none of these parameters varies significantly with fiber content.

Finally, also when the concrete was one year old, static flexural tests (EN 14651:2007) were performed. Table 2 shows the mean values of the strength at the limit of proportionality (f_L) and the maximum or ultimate strength (σ_{max}). It is observed that in all cases $\sigma_{max} > f_L$, which indicates that the post-peak strength due to the bridging forces of the fibers is higher than the first crack strength of the concrete; in other words, strain-hardening occurs. Moreover, as expected σ_{max} increases with fiber content.

2.3 Fatigue tests

A total of 12 fatigue tests per series were carried out, using notched prismatic specimens without pre-cracking (Figure 2).

Cycles with constant stress levels were applied until specimen failure occurred. To define the stress levels, in each series, the mean value of the maximum flexural strength (σ_{max}) was taken as a reference. Load cycles between 16% and 80% of σ_{max} were applied. Therefore, all series were subjected to the same relative stress levels, thus nullifying the effect of variations in static strength.

Table 2 lists the values of the stress levels S_{min} and S_{max} in each series.

Table 2: Mean LOP and maximum flexural strengths. Cyclic stress levels.

Series	f_L (MPa)	σ_{max} (MPa)	S_{max} (MPa)	S_{min} (MPa)
A1	7.36	8.78	7.02	1.40
A2	8.35	11.78	9.42	1.88
A3	10.45	19.65	15.72	3.14

The frequency of the load cycles was 5 Hz. Considering a design fatigue life of 10^4 cycles and an estimated scatter of about 2 orders of magnitude, the runout limit was set at 10^6 cycles.

The parameters measured in the tests were the load, the relative displacement between the lateral supports and the center section, and the crack opening (CMOD).

Figure 2: Flexural fatigue test.

2.4 Mesostructural study with microCT

All specimens tested under flexural fatigue were previously scanned by micro-computed tomography. For this purpose, a CoreTOM equipment (TESCAN, Brno, Czech Republic), which has a 300 W microfocus tube and a movable flat-panel detector, was used. The resolution achieved was 65 μm.

To obtain the geometrical properties of the steel fibers, the stacks of microCT images were postprocessed with image analysis techniques. Dragonfly open access software (ORS, Whitesboro, NY, USA) was used.

The most important step in this stage is the segmentation of the fibers; that is, the identification of the groups of voxels that correspond to each individual fiber. In the series with lower fiber content (series A1 and A2), it was sufficient to apply the thresholding technique, which basically consists of selecting the voxels whose gray level is in the range corresponding to the fibers. Complementarily, to solve some fiber grouping problems, it was combined with the watershed transform technique. However, the treatment of the A3 series was more complex. Due to the large volume of fibers, artifacts appeared that made segmentation difficult and resulted in clusters of many fibers that distorted the results. To solve this problem, an artificial intelligence model based on deep learning was generated into the software. The model adapts the fiber geometry to each voxel grouping, identifying and separating all individual fibers, even in environments where other techniques do not work properly.

Finally, once the fibers were segmented, their main geometrical parameters were calculated and exported: coordinates of the center of gravity, orientations, volume, length, etc.

3 RESULTS AND DISCUSSION

3.1 Fatigue life

Table 3 contains the fatigue lives of the 12 specimens of each series. It is worth mentioning that in all the tests of series A1 and in some of series A2, it is observed an initial fatigue phase in which the concrete is not cracked, of variable extension and characterized by small crack openings, less than 0.05 mm. As this mechanism is governed by the matrix and the fibers are hardly involved, the cycles associated with this phase were discarded. In this sense, one of the specimens of series A2 had an anomalous behavior, reaching the runout without having cracked. This test has not been taken into account.

Table 3: Cycles to failure in fatigue tests.

Test No.	A1	A2	A3
1	5,775	3,463	18,889
2	2,914	9,812	918
3	3,665	40,808	30
4	43	19,344	3,176
5	694	22,428	12,888
6	2,742	0*	7,195
7	7,108	26,252	15,225
8	3,629	20,746	12
9	1,495	5,156	31
10	4,329	5,068	3,090
11	1,710	14,233	3,743
12	48	5,024	2,219

Table 3 reveals that in all series there is a large dispersion of fatigue life. To facilitate the interpretation of the results, it is usual to fit the data to the two-parameter Weibull distribution function, expressed as (1):

$$F(x) = 1-\exp\{-(x/\lambda)^{\beta}\} \quad (1)$$

where x is log(N), β is the shape parameter and

λ is the scale parameter. The first is related to the dispersion, so that the larger β, the lower the variability of the results. The second is associated with the characteristic fatigue life, so that the higher the λ, the higher the fatigue life.

Figure 3 shows the Weibull fits to the N results for the three series. Table 4 contains the values of the fit parameters.

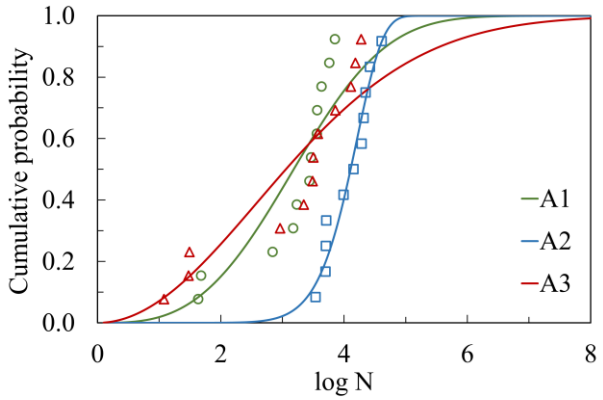

Figure 3: Weibull function fit to N.

Table 4: Parameters of Weibull function.

Series	λ	β	R^2
A1	3.58	3.11	0.80
A2	4.25	10.97	0.93
A3	3.67	2.01	0.86

Figure 3 and Table 4 indicate that series A2, with 0.6% fibers, has the longest fatigue life. The value of N for 0.5 probability is about 12,600 cycles. Series A1 and A3 show similar behaviors, with slightly lower fatigue lives. In this case, the values of N for 0.5 probability are about 1,600 and 1,300 cycles, respectively.

It is worth mentioning that in series A1 and A3 tests with a very low fatigue life, below 100 cycles, disturb the fit. In contrast, in series A2 there are no tests with such a low N, so the dispersion is very low, even for the usual in fatigue.

From the above, it is concluded that a higher fiber content does not necessarily lead to an improvement of the fatigue response. In fact, with the exception of the series A2, which has a statistically different behavior, the fatigue life in SFRC with 0.3% and 1% fiber contents remains practically the same.

3.2 Parameters based on cyclic creep curves

Fatigue life is a representative data, but it does not provide information on the damage evolution due to cyclic loading. For this purpose, it is interesting to study the cyclic creep curves, which represent the crack opening at the maximum stress level vs. the number of cycles [4,12]; in other words, the upper envelope of the CMOD vs. N diagram.

Figure 4 shows the cyclic creep curves of the tests of the three series. It can be seen that these curves have a characteristic S-shape, and are divided into three stages: (I) concrete cracking and fiber loading, (II) stable crack advance by progressive fiber failure, and (III) unstable crack propagation until global failure.

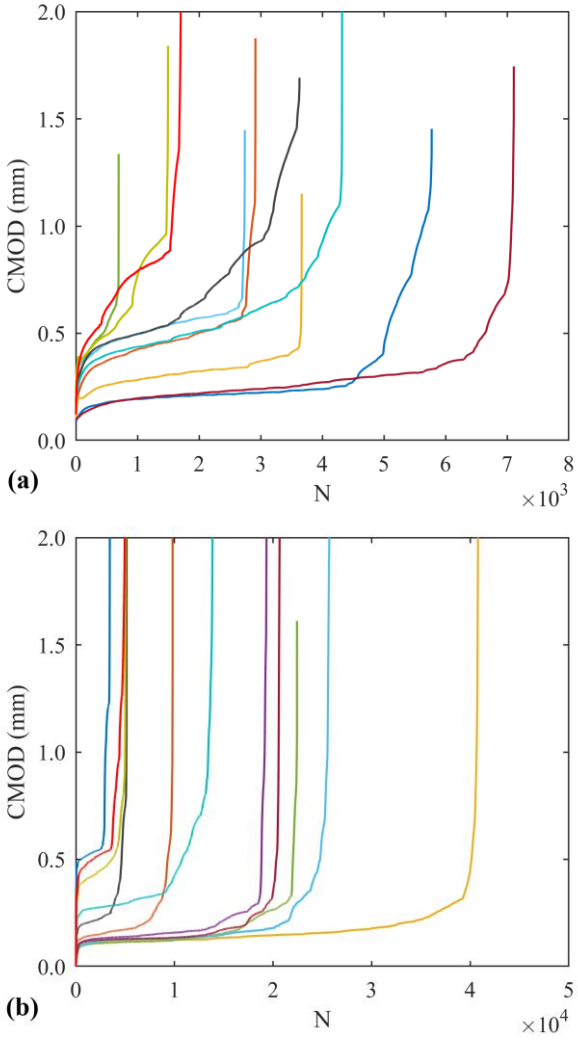

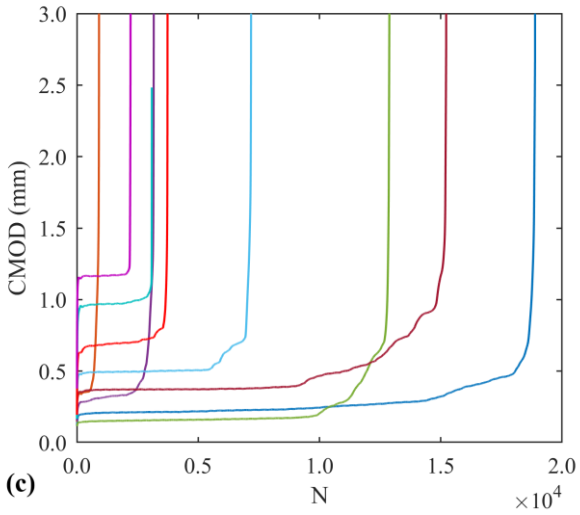

Figure 4: Cyclic creep curves in series A1 (a), A2 (b) and A3 (c).

Cyclic creep curves in Figure 4 may help to explain the large scatter in the results of N. Specifically, in this work, two parameters related to stage (II) are studied, since it is the most extensive and the one that governs the evolution of fatigue damage.

The first parameter is the slope of stage (II). Since this section is approximately linear, it can be fitted by least squares to a straight line, whose slope is called the secondary crack opening rate (dCMOD/dn) [5]. Figure 5 shows the linear regressions between the logarithms of N and dCMOD/dn for all series.

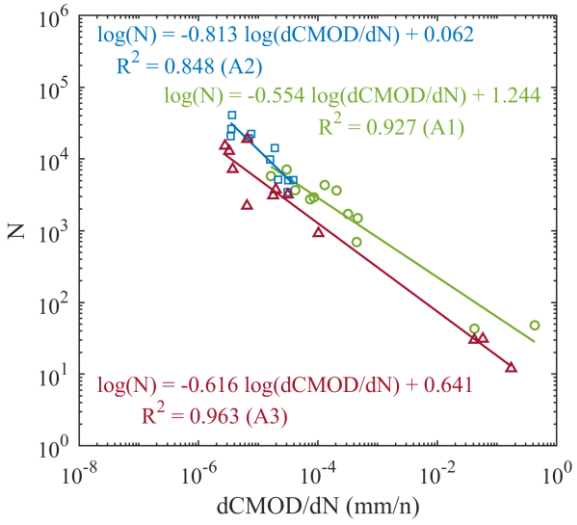

Figure 5: Linear regression between dCMOD/dn and N.

Figure 5 reveals that in all series there is a very good correlation between dCMOD/dn and N, so that the higher the dCMOD/dn, the lower the fatigue life. The values of the coefficient of determination R^2 range from 0.85 to 0.96.

As commented, this relationship was initially proposed in compressive fatigue [1], where it is well known and it is proved that, the higher the secondary strain rate (dε/dn), the lower is N. However, in flexural fatigue there are few works that address it in depth.

Therefore, it is concluded that the secondary crack opening rate is an adequate parameter to predict fatigue life. Figure 5 contains the formulas of the regression lines for the three series.

On the other hand, the second parameter that has been considered is the CMOD corresponding to the beginning of stage (II), called $CMOD_{II,i}$. The justification for the selection of this parameter is as follows. When the concrete cracks in stage (I), the CMOD stabilizes at a certain value, which marks the beginning of stage (II). This value depends on the distribution of fibers around the notch edge. It is proposed that the higher the $CMOD_{II,i}$, the smaller the effective cross-section of SFRC and therefore the earlier failure will be reached.

Figure 6 shows the linear regressions between the logarithms of N and $CMOD_{II,i}$ for all series.

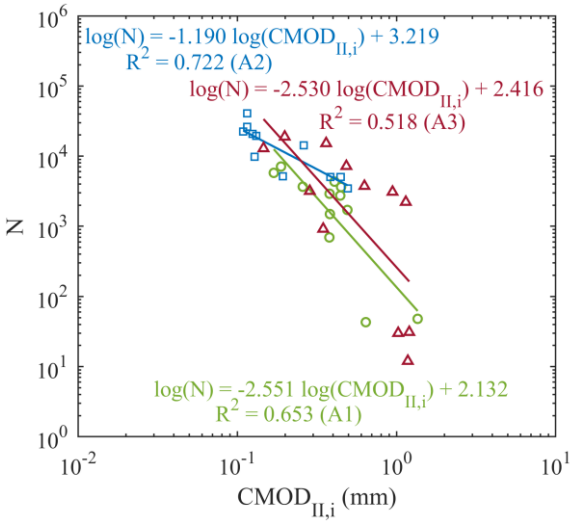

Figure 6: Linear regression between $CMOD_{II,i}$ and N.

Figure 6 shows that there is a good

correlation between $CMOD_{II,i}$ and N, confirming the hypothesis. However, R^2 values are lower than in the case of dCMOD/dn, being 0.65, 0.72 and 0.52 for series A1, A2 and A3, respectively.

The lower predictive capacity of this parameter may be due to the fact that it does not take into account the whole process of fatigue damage. It is possible that, although after cracking the $CMOD_{II,i}$ is very high, certain fiber accumulations at other points of the section may provide much strength and lead to higher fatigue lives. This seems to occur in the A3 series, which has the highest fiber content and the lowest R^2.

In any case, it is considered that this parameter can estimate the number of cycles to failure reasonably well, especially for SFRC with low and medium fiber contents. Figure 6 contains the formulas of the regression lines for the three series.

3.3 Parameters based on fiber arrangement

In this subsection, it is intended to explain the dispersion of fatigue results throughout the intact mesostructure of SFRC. In particular, correlations between the fatigue life and the geometrical parameters of the steel fibers are established.

It is worth mentioning that only the fibers located in the central 30 mm of the specimens (in longitudinal direction) have been considered; i.e., 15 mm on each side of the notch. This is because the flexural failure is local, and therefore the fibers in this region are the ones that can potentially influence the fatigue response.

Two fiber parameters have been considered: one related to orientation and the other to spatial distribution.

The orientation of the fibers of a specimen with respect to an axis can be characterized through the average of the angles they form, or by means of the so-called orientation efficiency indexes, or simply efficiency indexes [13]. They are expressed as (2):

$$ei_u = \sum(\cos \alpha_{u,i}) / n \qquad (2)$$

where u is the reference axis (X, Y or Z), $\alpha_{u,i}$ is the angle formed by each fiber with respect to the corresponding axis and n is the number of fibers in the study region.

The efficiency indexes take values between 0 and 1, where 1 indicates that all fibers are perfectly aligned with the reference axis, while 0 means that all are arranged perpendicular to it.

Figure 7 shows the linear regressions between the logarithm of N and the efficiency index on the Z-axis. The Z-axis is the axis normal to the midplane of the specimens (crack plane).

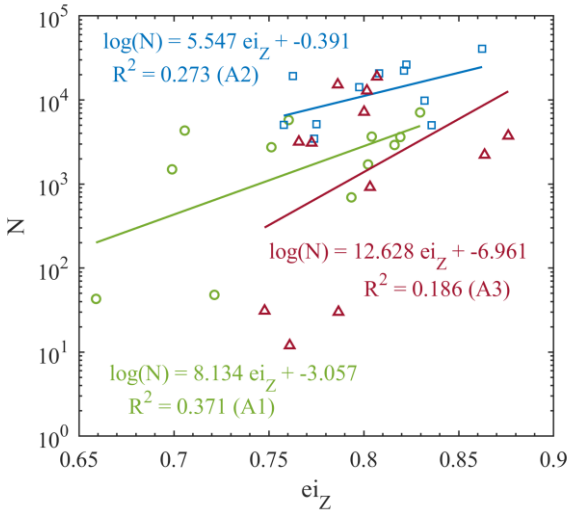

Figure 7: Linear regression between ei_Z and N.

Figure 7 reveals that in all series there is a certain correlation between fiber orientation and N. Higher values of ei_Z lead to longer fatigue lives. This is because, when the fibers are more perpendicular to the crack plane, the bridging forces they generate are higher, increasing the strength against cyclic loading.

The best fit is obtained for series A1, with an R^2 of 0.37. In general, the coefficients of determination are low, indicating that the efficiency index cannot explain by itself the dispersion of N. Be that as it may, in all series the trends are clear, so it can be stated that the influence of ei_Z on fatigue life is not negligible. Figure 7 contains the formulas of the linear regression models that allow estimating N.

On the other hand, another parameter that can affect the dispersion of the fatigue response is the density of fibers passing

through the midplane of the specimens (fibers / mm^2). However, since in this case SFRCs with different fiber contents are compared, it is proposed to use a normalized parameter called relative fiber density ($\rho_{fib,rel}$), expressed as (3):

$$\rho_{fib,rel} = \rho_{fib} / \rho_{fib,m} \quad (3)$$

where ρ_{fib} is the fiber density of the specimen considered and $\rho_{fib,m}$ is the average fiber density of the series to which it belongs.

Figure 8 shows the linear regressions between the logarithm of N and $\rho_{fib,rel}$.

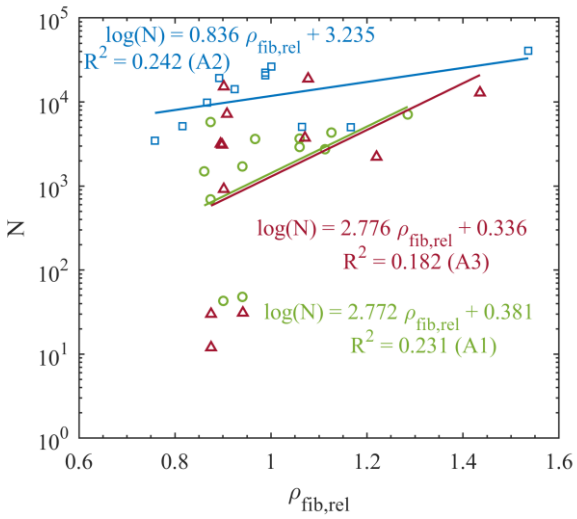

Figure 8: Linear regression between $\rho_{fib,rel}$ and N.

Figure 8 shows that as the density of fibers passing through the midplane increases, so does the fatigue life. Again, the R^2 coefficients are low, taking values of 0.23, 0.24 and 0.18 for series A1, A2 and A3, respectively. Although the correlations are not very robust, the trends are visible and are also similar in the three series. In fact, the regression lines in series A1 and A3 are practically coincident.

Consequently, this proves that, within each series, small variations in the fiber distribution can explain, at least partially, the dispersion of the fatigue life observed.

4 CONCLUSIONS

In this work, two types of parameters are proposed to estimate the flexural fatigue life in SFRC. On the one hand, macrostructural indicators based on cyclic creep curves. On the other hand, parameters related to the mesostructure of the intact specimens, specifically to the fibers. The main conclusions are summarized below:

- In cyclic creep curves, it is shown that the secondary strain rate is a very suitable parameter to estimate the fatigue life. It is found that there is a very good correlation between dCMOD/dn and N in all series. On the other hand, the CMOD corresponding to the beginning of stage (II), called $CMOD_{II,i}$, also explains the dispersion of the results. However, its predictive capacity is lower than that of dCMOD/dn, which is attributed to the fact that it does not take into account the entire damage evolution process.
- With respect to the geometrical properties of the fibers, it is observed that both the efficiency index in the Z-axis (ei_Z) and the relative density of fibers crossing the crack plane ($\rho_{fib,rel}$) have a certain correlation with N. It is noted that the higher ei_Z and $\rho_{fib,rel}$, the higher the fatigue life. However, the fits are not very robust, which points to the fact that neither of these two parameters is able to explain the dispersion of fatigue life on its own. It is likely that multiple regression models combining these parameters can more accurately estimate the variability of the results.
- The results demonstrate that macroscopic damage parameters based on cyclic creep curves are better predictors of fatigue response than those related to fiber arrangement in intact specimens. However, it should be emphasized that the advantage of the latter is that they can be determined without inflicting prior fatigue damage. They can therefore be used preliminarily to reduce, at least partially, the large initial scatter.

REFERENCES

[1] P.R. Sparks, J.B. Menzies, The effect of rate of loading upon the static and fatigue strengths of plain concrete in compression, Mag. Concr. Res. 25 (1973) 73–80. https://doi.org/10.1680/macr.1973.25.83.73.

[2] L. Saucedo, R.C. Yu, A. Medeiros, X. Zhang, G. Ruiz, A probabilistic fatigue model based on the initial distribution to consider frequency effect in plain and fiber reinforced concrete, Int. J. Fatigue. 48 (2013) 308–318. https://doi.org/10.1016/j.ijfatigue.2012.11.013.

[3] E. Poveda, G. Ruiz, H. Cifuentes, R.C. Yu, X. Zhang, Influence of the fiber content on the compressive low-cycle fatigue behavior of self-compacting SFRC, Int. J. Fatigue. 101 (2017) 9–17. https://doi.org/10.1016/j.ijfatigue.2017.04.005.

[4] D.M. Carlesso, A. de la Fuente, S.H.P. Cavalaro, Fatigue of cracked high performance fiber reinforced concrete subjected to bending, Constr. Build. Mater. 220 (2019) 444–455. https://doi.org/10.1016/j.conbuildmat.2019.06.038.

[5] F. Germano, G. Tiberti, G. Plizzari, Post-peak fatigue performance of steel fiber reinforced concrete under flexure, Mater. Struct. 49 (2016) 4229–4245. https://doi.org/10.1617/s11527-015-0783-3.

[6] Ł. Skarżyński, J. Suchorzewski, Mechanical and fracture properties of concrete reinforced with recycled and industrial steel fibers using Digital Image Correlation technique and X-ray micro computed tomography, Constr. Build. Mater. 183 (2018) 283–299. https://doi.org/10.1016/j.conbuildmat.2018.06.182.

[7] B. Zhou, Y. Uchida, Influence of flowability, casting time and formwork geometry on fiber orientation and mechanical properties of UHPFRC, Cem. Concr. Res. 95 (2017) 164–177. https://doi.org/10.1016/j.cemconres.2017.02.017.

[8] G.L. Balázs, O. Czoboly, É. Lublóy, K. Kapitány, Á. Barsi, Observation of steel fibres in concrete with Computed Tomography, Constr. Build. Mater. 140 (2017) 534–541. https://doi.org/10.1016/j.conbuildmat.2017.02.114.

[9] M.A. Vicente, G. Ruiz, D.C. González, J. Mínguez, M. Tarifa, X. Zhang, Effects of fiber orientation and content on the static and fatigue behavior of SFRC by using CT-Scan technology, Int. J. Fatigue. 128 (2019) 105178. https://doi.org/10.1016/j.ijfatigue.2019.06.038.

[10] M.A. Vicente, J. Mínguez, D.C. González, Computed tomography scanning of the internal microstructure, crack mechanisms, and structural behavior of fiber-reinforced concrete under static and cyclic bending tests, Int. J. Fatigue. 121 (2019) 9–19. https://doi.org/10.1016/j.ijfatigue.2018.11.023.

[11] Ł. Skarżyński, I. Marzec, J. Tejchman, Fracture evolution in concrete compressive fatigue experiments based on X-ray micro-CT images, Int. J. Fatigue. 122 (2019) 256–272. https://doi.org/10.1016/j.ijfatigue.2019.02.002.

[12] G.A. Plizzari, S. Cangiano, S. Alleruzzo, The fatigue behaviour of cracked concrete, Fatigue Fract. Eng. Mater. Struct. 20 (1997) 1195–1206. https://doi.org/10.1111/j.1460-2695.1997.tb00323.x.

[13] M.A. Vicente, Á. Mena, J. Mínguez, D.C. González, Use of Computed Tomography Scan Technology to Explore the Porosity of Concrete: Scientific Possibilities and Technological Limitations, Appl. Sci. 11 (2021) 8699. https://doi.org/10.3390/app11188699.